Latvian Journal of Chemistry, No 1, 2014, 28–40
DOI: 10.2478/ljc-2013-0003

CHARACTERIZATION AND PHYSICOCHEMICAL EVALUATION OF MOLECULAR COMPLEXES FORMED BETWEEN UMIFENOVIR AND DICARBOXYLIC ACIDS

A. Kons[1], A. Bērziņš[1,2], K. Krūkle-Bērziņa[1], A. Actiņš[1]

[1] Faculty of Chemistry, University of Latvia, Krišjāņa Valdemāra iela 48, Riga, Latvia, LV-1045
[2] Department of Chemistry, Durham University, South Road, Durham, UK, DH1 3LE
e-mail: artis.kons@gmail.com

The paper reports the investigation of three umifenovir molecular complexes with dicarboxylic acids, prepared to improve the bioavailability of this drug. All three molecular complexes were investigated by powder X-ray diffraction, infrared spectroscopy, and solid-state nuclear magnetic resonance spectroscopy. The solubility and thermal properties were determined as well. Polymorph and solvate screening of umifenovir molecular complexes were performed by recrystallization from various solvents, as well as neat and solvent-drop grinding.

Key words: *umifenovir, molecular complexes, polymorph and solvate screening.*

INTRODUCTION

It is known that different polymorphs or pseudopolymorphs of pharmaceutical compounds may possess different chemical and physical properties which can affect the bioavailability and stability of the resulting drugs [1–3]. Crystalline form screening is a common procedure during the development of pharmaceutical molecules, and it is often possible to obtain drug candidates as many types of crystal forms, including salts, polymorphs, solvates (typically hydrates), and co-crystals [4].

Salt formation is a common approach to improve the solubility of poorly soluble drugs [5]. About 40% of commercially marketed pharmaceutical salts are hydrochlorides. The selection of chloride as a counterion has advantages over other salt forming anions because of its low molecular weight and low toxicity. However, hydrochloride salts can have some undesirable issues, such as a decreased solubility in stomach due to common ion effects with physiologically occurring chloride ions [6]. A new trend in pharmaceutical research is the design of co-crystals to improve solid drug properties. The distinction between co-crystals and salts is based on the fact that co-crystals are complexes between two neutral, hydrogen-bonded molecular entities that coexist as molecules in solution, whereas salts are ionic compounds where a proton transfer from acid to base has occurred, and ions are found in the solution phase [7].

A variety of techniques have been employed to characterize the solid forms of pharmaceuticals, including X-ray diffraction (XRD), thermal analysis (differential scanning calorimetry (DSC), thermogravimetry (TG), differential

thermal analysis (DTA)), solid state nuclear magnetic resonance (ssNMR) spectroscopy, optical microscopy, and vibrational spectroscopy (including infrared (IR) and Raman spectroscopy) [8].

Umifenovir is 1-methyl-2-phenylthiomethyl-3-ethoxycarbonyl-4-dimethylaminomethyl-5-hydroxy-6-bromoindole (Fig. 1), used as an antiviral medication for the treatment of influenza A and B infections. Umifenovir as a free base is practically insoluble in water, therefore umifenovir hydrochloride monohydrate has been developed as a commercially available drug, and has been marketed under the brand name Arbidol®. The disadvantage of Arbidol® is its low bioavailability, where approximately 40% of umifenovir is excreted with feces [9]. This paper focuses on the potential use of umifenovir molecular complexes to improve its physicochemical properties. The physicochemical properties of maleate, fumarate, and succinate were compared to those of the free base and hydrochloride monohydrate.

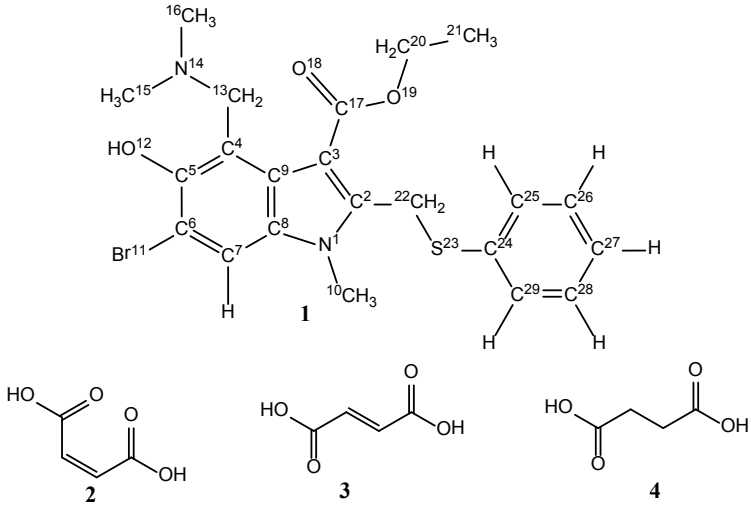

Fig. 1. The molecular structures of (1) umifenovir base with atom numbering and the dicarboxylic acids used in this study: (2) maleic acid, (3) fumaric acid, and (4) succinic acid.

EXPERIMENTAL

Materials

A pharmaceutical grade sample of umifenovir hydrochloride monohydrate was obtained from JSC Grindeks (Latvia, Riga). The purity with respect to polymorphic forms was evaluated using PXRD by comparing to the theoretical diffraction pattern simulated from crystal structure data [10].

Maleic acid, fumaric acid, succinic acid, acetone, ethyl acetate, methanol, ethanol, 2-propanol, n-butanol, tetrahydrofuran, toluene, dichloromethane, chloroform, N,N-dimethylformamide and dimethyl sulphoxide were procured from commercial suppliers and were used without further purification.

The umifenovir base was obtained from umifenovir hydrochloride monohydrate by dissolving 10.0 g (18.8 mmol) of umifenovir hydrochloride monohydrate in 200 mL of deionized water, followed by heating and stirring of the obtained mixture. After complete dissolution, a solution of 0.75 g (18.8 mmol) NaOH in 20 mL deionised water was added to the umifenovir hydrochloride solution. The precipitate of umifenovir base was filtered and air

dried [11]. For phase identification of the obtained product PXRD was used, and the results were compared to the diffraction pattern simulated from crystal structure data [10].

Umifenovir base (0.500 g, 1.05 mmol) and 1.05 mmol of a dicarboxylic acid (either maleic acid (0.122 g) or fumaric acid (0.122 g), or succinic acid (0.124 g)) were dissolved in 20 mL of hot acetone and allowed to crystallize by evaporating the solvent in 22±1°C temperature . For phase identification of the obtained product PXRD was used by comparing the diffraction patterns to those of the free base and the corresponding dicarboxylic acid.

The PXRD patterns were determined on a Bruker D8 Advance diffractometer using copper radiation (CuK_α = 1.54180 Å) with Bregg-Brentano geometry and LynxEye (1D) detector. The tube voltage and current were set to 40 kV and 40 mA, respectively. The divergence and antiscattering slits were set at 0.6 mm, and the receiving slit was set at 8 mm. The patterns were recorded from 3° to 30° on the 2θ scale, using a scan speed of 0.2s/0.02.

Differential thermal analysis/thermogravimetric analysis were performed with an Exstar6000 TG/DTA6300 (SII) instrument. Open aluminium pans were used. Heating of samples from 30 °C to 220 °C was performed at the heating rate of 10 °C·min^{-1} under a 100 mL·min^{-1} nitrogen flow. The sample mass was approximately 5–7 mg.

Differential scanning calorimetry analyses were performed with a DSC 823e instrument (Mettler Toledo). The pinholed aluminium pans with 0.5 mm hole diameter were used. Heating of samples from 30 °C to 220 °C was performed at the heating rate of 10 °C·min^{-1}. The sample mass was approximately 7 mg.

Attenuated Total Reflectance Fourier Transform Infrared Spectroscopy (ATR-FTIR) spectra were obtained with a PerkinElmer Frontier FTIR spectrometer with a Universal ATR Sampling Accessory attachment. A background spectrum was recorded before each sample, and a small amount of powder was placed on the ATR diamond crystal. The spectra were recorded over the range of 4000–650 cm^{-1} with a 2 cm^{-1} resolution, and 20 scans per sample were summed.

High-resolution solid-state NMR spectra were acquired at 20°C temperature using a Bruker Avance III HD spectrometer (Bruker, Karlsruhe, Germany), operating at 125.67 MHz for ^{13}C (499.72 MHz for ^{1}H) with a 4.0 mm (rotor outside diameter) magic angle spinning (MAS) probe. Spectra were obtained under the MAS conditions using cross polarization (CP) with the following conditions: recycle delay 5 s, contact time 1-2 ms, acquisition time 30 ms, and a sample spin rate of 13 kHz. The spectra were referenced with respect to external neat TMS for ^{13}C by setting the high-frequency signal from a replacement sample of adamantane to 38.4 ppm.

The chemical shift calculations were carried out with the GIPAW method implemented in CASTEP [12–15]. The crystal structures of umifenovir salts and the free base were obtained from the literature [10, 11] and geometry optimization was performed in CASTEP. All calculations were performed with the PBE [16] functional using *on-the-fly* generated ultrasoft pseudopotentials and a cut-off energy of 600 eV. For geometry optimization two approaches were used – optimization of only the hydrogen atom positions, and optimization of all atom positions. The unit cell parameters in both cases were fixed to the

values determined from X-ray diffraction studies. The computed ^{13}C chemical shifts were referenced by fitting the computed shielding values to the experimental chemical shifts. By using the crystal structures of umifenovir maleate, glutarate, and salicylate with optimized geometries, the theoretical co-crystal structures for chemical shift calculation were prepared by proton transfer from the protonated N14 nitrogen atom to the carboxylate anion moiety. Geometry optimization of these structures was not suitable for our study because it resulted in formation of the initial experimental salt structures.

The solubilities of umifenovir fumarate and succinate were determined in water at 22 ± 1°C temperature. An excess of each polymorphic form of these salts was suspended in 30 mL of deionized water, and the suspensions were agitated by shaking for 24 h in closed vessels. The salt solution concentrations were determined with a Lambda 25 UV-Vis spectrophotometer (PerkinElmer) using 1.0 cm quartz cuvettes. The UV-Vis absorption spectra for all samples were recorded in the range from 190 to 400 nm. The absorbance measurements of salt solutions were performed at 218 nm for fumarate A, at 215 nm for fumarate B (see chapter 3.5.), and at 223 nm for the succinate. All UV-Vis measurements were performed in triplicate. A separate linear calibration curve was plotted for each salt. After solubility determination the composition of the solid phase was analyzed by PXRD in order to detect any possible phase changes.

Recrystallization of umifenovir maleate, fumarate, and succinate was performed from the following solvents: acetone, acetone-water mixture, ethyl acetate, methanol, ethanol, 2-propanol, *n*-butanol, tetrahydrofuran, toluene, dichloromethane, chloroform, *N,N*-dimethylformamide, and dimethyl sulphoxide. Hot saturated solutions were prepared, filtered, and allowed to crystalize at ambient conditions, then the crystallized solids were examined by PXRD. The TG/DTA data were used to determine if the new crystalline phases were polymorphs or solvates.

Neat and solvent-drop grinding experiments were performed at ambient conditions in a ball mill with 15 Hz frequency for 10 minutes. Cylindrical stainless steel jar (internal volume =5 mL) and one stainless steel ball (diameter =0.9 cm) were used to grind a 1:1 mixture of umifenovir base with a dicerboxylic acid, and identical grinding conditions were repeated for each experiment, with the exception of the solvent addition for solvent-drop grinding. For solvent-drop grinding 2 drops (~0.15 mL) of the following solvents were used: water, acetone, ethyl acetate, methanol, ethanol, 2-propanol, *n*-butanol, tetrahydrofuran, toluene, dichloromethane, chloroform, *N,N*-dimethylforma-mide, and dimethyl sulphoxide. Analysis by PXRD was used to determine the existence of new crystalline phases and TG/DTA was used to determine if the new crystalline phases were polymorphs or solvates.

RESULTS AND DISCUSSION

The PXRD patterns were used to identify new crystalline phases. The PXRD patterns of newly crystallized umifenovir forms were compared to those of the free base and the corresponding acid. The newly obtained umifenovir crystal

forms had PXRD patterns with distinct features (Fig. 2). These results suggested that the products obtained in crystallization experiments with fumaric acid or succinic acid were umifenovir salts or co-crystals. For phase identification of umifenovir maleate, the PXRD pattern of the obtained product was compared to a diffraction pattern simulated from crystal structure data [11]. The good match of both patterns confirmed the formation of umifenovir maleate in the crystallization experiment.

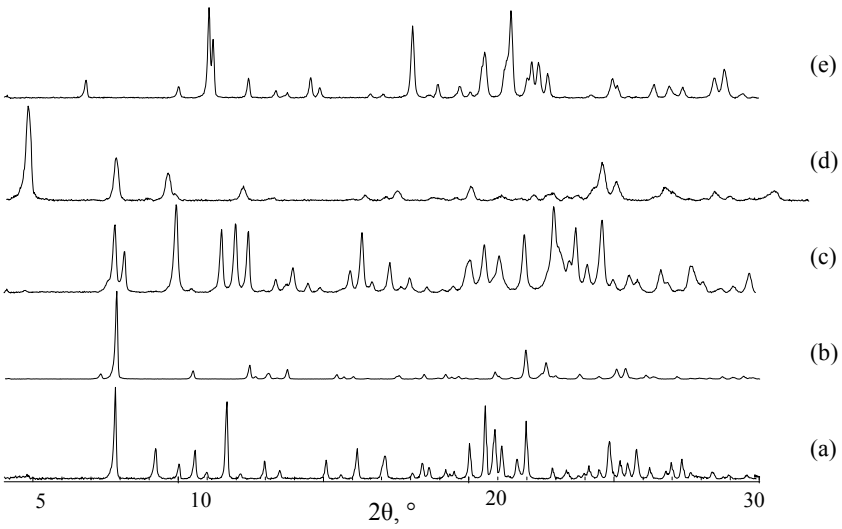

Fig. 2. The PXRD patterns of umifenovir crystal forms:
(a) succinate, (b) maleate, (c) fumarate, (d) hydrochloride monohydrate, and (e) the free base.

The negative common logarithm of acid ionisation constant (pK_a) is a commonly used tool for predicting the ionization states of molecular species in solid forms, despite the fact that pK_a values are only valid under the solution equilibrium conditions at which they were determined [7]. The situations where ΔpK_a (the pK_a difference between the base and acid) is larger than 3 almost exclusively result in salt formation, while situations with $\Delta pK_a<0$ almost exclusively result in cocrystal formation, but $0<\Delta pK_a<3$ can lead to either salts or co-crystals, or even complexes with partial proton transfer, with the location of the acidic proton dependent on the specific crystal packing environment [17]. Table 1 presents the ΔpK_a values calculated from the pK_a values of umifenovir and dicarboxylic acids given in the literature [18].

Table 1. **The pK_a values of dicarboxylic acids, with the derived ΔpK_a values**

Molecular complex	Dicarboxylic acid	pK_a	ΔpK_a
Umifenovir maleate	Maleic acid	1.83	4.2
Umifenovir fumarate	Fumaric acid	3.03	3.0
Umifenovir succinate	Succinic acid	4.16	1.8

The pK_a value of the umifenovir base has been reported to be 6.0 [19]. Thus, the ΔpK_a value of maleate (4.2) and fumarate (3.0) suggest salt formation, but the ΔpKa of succinate (1.8) allows for some ambiguity with regard to the nature of this complex.

By using FTIR spectroscopy, the instances of salt formation could be confirmed by the presence of bands characteristic of carboxylic acid salts at 1650–1550 and 1440–1335 cm^{-1} [20]. An additional indicator for a salt formation with the acid component can be a shift of the umifenovir C=O IR absorption band. The carbonyl band wavenumber (cm^{-1}) of protonated umifenovir was the same or slightly higher than that of the free base, whereas a slight decrease in wavenumber occurred for co-crystals [21, 22].

The presence of characteristic bands at 1555 and 1385 cm^{-1} in umifenovir maleate and fumarate IR spectra indicated that maleate and fumarate were salts, while the absence of these bands in umifenovir succinate spectra indicated that it was a cocrystal. The C=O band in both maleate and fumarate IR spectra remained in the same position as the C=O band given by the free base of umifenovir (Table 2), providing a further indication that these molecular complexes were salts, while in umifenovir succinate the C=O band exhibited a shift to lower wavenumbers, suggesting that succinate was a cocrystal.

Table 2. **The C_{17}=O band positions in the ATR-IR spectra of umifenovir free base and some molecular complexes**

Compound	$\tilde{\nu}$ (C_{17}=O stretch), cm^{-1}
Umifenovir free base	1689 ± 2
Umifenovir hydrochloride monohydrate	1688 ± 2
Umifenovir fumarate	1689 ± 2
Umifenovir maleate	1687 ± 2
Umifenovir succinate	1676± 2

In order to further investigate the possible proton transfer in molecular complexes of umifenovir, the fumarate, maleate, succinate, and the free base of umifenovir were characterized by solid-state NMR spectroscopy. Chemical shift calculations for umifenovir maleate and base were performed to assign the peaks. Calculations for other umifenovir salts (salicylate, hydrochloride, and glutarate) were performed to better understand the connection between chemical shifts and the chemical environment of the molecular entities in the solid state.

The ^{13}C CPMAS spectra of the analysed umifenovir crystalline forms are given in the Fig. 3. The assignment of the peaks for maleate and base was performed based on the CASTEP calculations (see Fig. 1 for atom numbering in umifenovir). The chemical shifts calculated after optimization of all atom positions gave a better agreement to the experimental spectra than those calculated after optimizing only the hydrogen atoms, so these results were further used and the calculated spectra are given in the Fig. 3. After rescaling the calculated chemical shifts based on the performed regression analysis with experimental data, the root-mean-square deviations between the calculated and

experimental chemical shifts were respectively 1.32 and 1.12 for umifenovir maleate and base, thus showing a good agreement with the experimental spectra [23, 24].

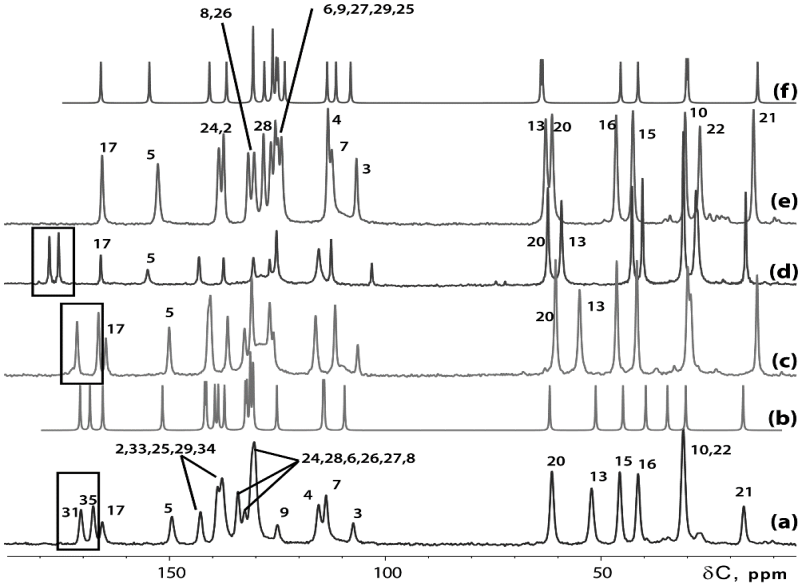

Fig. 3. The experimental ^{13}C CPMAS spectra of (a) umifenovir maleate, (c) fumarate, (d) succinate, and (e) free base, as well as the calculated spectra of (b) umifenovir maleate and (f) free base.

Based on the experimentally obtained spectra and performed calculations, it was possible to assign some of the peaks in umifenovir fumarate and succinate, which could be used to distinguish between the salt or co-crystal character (Fig. 3). First, it was determined that signals from C20, C17, and C5 in all spectra should be in the same place. Second, the closest signal to C20 was always the signal from C13 of the methylene group next to the N14 nitrogen atom that was protonated in the salts. Thus, the position of this signal was likely to be dependent on the nitrogen protonation state. The experimental and calculated positions of this peak are given in Table 3. Third, in molecular complexes with dicarboxylic acids the signals with the highest chemical shifts (marked with rectangles) corresponded to the carboxyl or carboxylate groups of the acids.

Table 3. **The experimental and calculated chemical shift values for C13 in umifenovir molecular complexes.**

	δ(C13), ppm	
Compound	**Experimental**	**Calculated**
Umifenovir maleate	52.3	51.2
Umifenovir fumarate	55.0	-
Umifenovir succinate	59.2	-
Umifenovir free base	62.9	63.8

It was determined that downfield chemical shifts of the C13 carbon atom correlated with an unprotonated N14 nitrogen atom. This was supported by the performed calculations, as well as by the experimental measurements. These measurements were in accordance with the pK_a differences and with the performed IR spectroscopy measurements, and suggested that umifenovir succinate was cocrystal, whereas fumarate most probably was a salt. Nevertheless, the chemical shift of C13 atom in umifenovir succinate spectrum was downfield relative to the C13 signal in umifenovir maleate spectrum, which could suggest that the succinic acid in this crystal was not as completely deprotonated as maleic acid in umifenovir maleate that has shown a salt character with all the methods used and was proved to be a salt by X-ray structural analysis [11]. Although the calculations indicated that in co-crystals at least one of the dicarboxylic acid carboxyl groups should give a ^{13}C signal that is shifted downfield and both salts had upfield carboxyl group ^{13}C signals compared to umifenovir succinate, calculations of chemical shifts in umifenovir glutarate suggested that this most probably was associated with the absence of double bond between the carboxyl groups. A similarity between the umifenovir salts and between the umifenovir base and succinate was observed in the position of the C5 signal. However, this can be associated with either the protonation state of the N14 nitrogen atom or differences in hydrogen bonding, thus conclusions could not be drawn without a knowledge of umifenovir succinate crystal structure. In order to fully confirm the protonation state of the nitrogen atom, ^{15}N solid-state NMR spectra could be used [22, 25, 26].

DSC and TG measurements were performed to investigate the thermal properties of umifenovir maleate, fumarate, and succinate, and to compare these properties to those of the free base and hydrochloride monohydrate. The DSC curves showed different melting peaks, which were observed at 128 °C for the free base, 189 °C for the hydrochloride monohydrate, 146 °C for the fumarate, 136 °C for the maleate, and 141 °C for the succinate (Fig. 4).

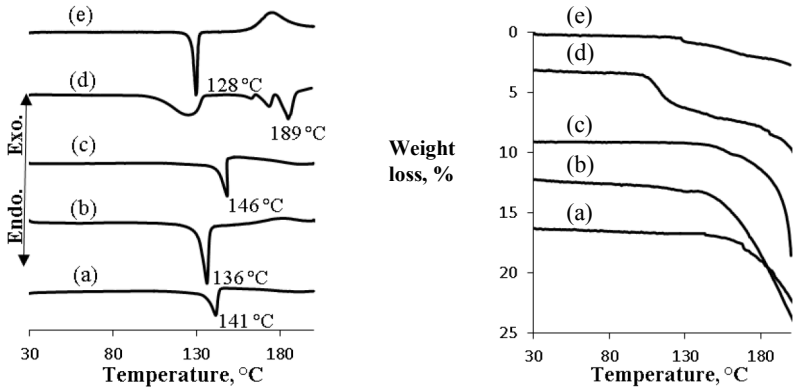

Fig. 4. The DSC and TG curves of umifenovir crystal forms:
(a) succinate, (b) maleate, (c) fumarate, (d) hydrochloride monohydrate, and (e) free base.

The TG curves of fumarate, maleate, and succinate showed that there was no weight loss before melting (Fig. 4), suggesting that the prepared crystals were not solvates. Each umifenovir crystal form showed a different decomposition

temperature, which was detected as the beginning of weight loss after the melting, depending on the dicarboxylic acids.

Studies have been carried out to investigate the relationship between certain physicochemical properties of salts, like solubility and melting point, melting point and enthalpy of fusion, as well as the melting point of a salt and that of the corresponding acid, and other combinations of properties [27–29]. The solubility values of umifenovir molecular complexes, the melting points determined from the maximum of the endothermic peak, and the enthalpy of fusion were determined and are given in Table 4 together with the literature values for the melting points of the corresponding acids [18].

Table 4. **The physicochemical properties of umifenovir molecular complexes and the free base of umifenovir.**

Compound	Melting point, °C	Enthalpy of fusion, $kJ \cdot mol^{-1}$	Corresponding acid melting point, °C	Solubility, $mg \cdot mL^{-1}$
Umifenovir free base	126	38.8	-	0.04±0.01
Umifenovir hydrochloride monohydrate	179	28.4	-	2.2±0.1
Umifenovir fumarate	146	34.4	287	0.7±0.1
Umifenovir succinate	141	39.2	184	0.8±0.1
Umifenovir maleate	136	40.9	135	2.7±0.1[11]

There is a good correlation between the enthalpy of fusion and melting point of umifenovir complexes with dicarboxylic acids: a decrease in molecular complex melting point accompanies an increase in the enthalpy of fusion. The results also show that the formation of multiple complexes with acids increased the melting points of the respective umifenovir crystal forms, and an increase in the corresponding acid melting point also increased the melting point of a molecular complex. No direct relationship between the melting point and solubility was observed for these umifenovir molecular complexes. The salts with the lowest melting points had the highest solubility, but the salt with the second highest solubility had the highest melting point.

As can been seen from Table 4, umifenovir fumarate and succinate has the lowest solubility and therefore offers a potential to decrease the amount of umifenovir excreted from the human body in an unchanged form.

Results of the recrystallization experiments, as determined by PXRD, DSC, and TG/DTA analysis, are summarized in Table 5. Recrystallization of umifenovir maleate from toluene and acetone with water as anti-solvent resulted in the formation of umifenovir maleate toluene hemisolvate and a non-stoichiometric umifenovir maleate hydrate (the highest possible water content 3.5–4.1%), respectively. Both of these new umifenovir maleate crystalline forms were desolvated by forming the thermodynamically stable form when stored for one month at ambient conditions.

Recrystallization of umifenovir fumarate from ethanol, THF, DMSO, and DMF produced a new polymorph (B). The new polymorphic form had a melting

point of 160°C and melting enthalpy of 16.6 $kJ \cdot mol^{-1}$, therefore showing that both polymorphic forms were enantiotropically related. Solubility measurements showed that the form A had a lower solubility than the form B (1.1 $mg \cdot mL^{-1}$), and thus the form A was the thermodynamically stable form at ambient temperature. A mixture of both polymorphs appeared if fumarate was recrystallized from ethyl acetate, methanol, 2-propanol, toluene, or chloroform. Decomposition of umifenovir fumarate was observed in dichloromethane.

Recrystallization of umifenovir succinate did not produce any new crystalline forms. Decomposition of this molecular complex was observed in *N,N*-dimethylformamide, dimethyl sulphoxide, and partially in ethanol as well.

Table 5. **The phases obtained after recrystallization of umifenovir molecular complexes (1 – the form thermodynamically stable in standard conditions)**

Crystallization solvent	Umifenovir maleate	Umifenovir fumarate	Umifenovir succinate
Acetone	1	A	1
Ethyl acetate	1	A+B	1
Methanol	1	A+B	1
Ethanol	1	B	1+Base
2-Propanol	1	A+B	1
n-Butanol	1	A	1
Tetrahydrofuran	1	B	1
Toluene	½ T solvate	A+B	1
Dichloromethane	1	Base	1
Chloroform	1	A+B	1
N,N-Dimethylformamide	1	B	Base
Dimethyl sulphoxide	1	B	Base
Acetone with anti-solvent water	Hydrate	Hydrate + B	1

The decomposition of umifenovir fumarate was probably caused by the different pK_a of fumaric acid in dichloromethane, but succinate as cocrystal was less stable than umifenovir salts in these solvents, because its decomposition did not involve a proton transfer.

Results of the mechanochemical screening experiments applied to the molecular complexes of umifenovir, as determined by PXRD and TG/DTA analysis, and summarized in Table 6, demonstrated several possible outcomes due to grinding: either no reaction, as evaluated by the presence of starting materials in a physical mixture; same crystalline forms as obtained by crystallization; or a new crystalline forms.

Umifenovir maleate acetone hemisolvate was obtained by solvent drop grinding of umifenovir base and maleic acid with acetone. Maleate acetone hemisolvate was desolvated, producing the thermodynamically stable form over one week at ambient conditions. Umifenovir fumarate dihydrate and chloroform

hemisolvate were obtained by solvent drop grinding of umifenovir base and fumaric acid with water and chloroform, respectively. Fumarate dihydrate was stable at the relative humidity above 40% at ambient temperature. At the relative humidity below 40% the dihydrate was dehydrated to a new crystalline form-fumarate monohydrate, which then dehydrated at 50°C to the polymorph B. The fumarate chloroform hemisolvate was desolvated by producing the fumarate form A over one week at ambient conditions.

Table 6. **The phases obtained after neat and solvent-drop grinding of umifenovir with dicarboxylic acids (1 – the form thermodynamically stable at standard conditions)**

Solvent-drop grinding	**Umifenovir maleate**	**Umifenovir fumarate**	**Umifenovir succinate**
Water	1	Dihydrate	1
Acetone	½ A solvate	A+B	1
Ethyl acetate	1	A+B	1
Methanol	1	A+B	1
Ethanol	1	B	1
2-Propanol	1	A	1
n-Butanol	1	A	1
Tetrahydrofuran	1	A+B	1
Toluene	½ T solvate	A+B	1
Dichloromethane	1	A+B	1
Chloroform	1	½ C solvate	1
N,N Dimethylformamide	1	A+B	1
Dimethyl sulphoxide	1	A+B	1
Neat grinding	Base+ amorphous	Base+ amorphous	Base+ amorphous

CONCLUSIONS

Two new umifenovir molecular complexes (succinate and fumarate) have been prepared for the first time and one known molecular complex (maleate) has been obtained by a literature method.

The investigation by ATR-FTIR and ^{13}C ssNMR spectroscopy methods showed that umifenovir fumarate was a salt, while the succinate most probably was a co-crystal, in agreement to the calculated ΔpK_a value and its low stability in various solvents.

The crystal form screening of umifenovir molecular complexes showed that two solvates of maleate can exist (with acetone and toluene), while the fumarate can exist as two enantropically related polymorphs and three solvates (dihydrate, monohydrate, and chloroform solvate), whereas succinate has only a single form.

Investigation showed that it is possible to change the bioavailability of umifenovir by changing its salt form, as evaluated from the different solubility of umifenovir molecular complexes.

Acknowledgments

This work was supported by the European Regional Development Fund (Grant No. 2011/0014/2DP/2.1.1.1.0/10/APIA/VIAA/092).

R E F E R E N C E S

1. Brittain, H.G. (2011). Polymorphism and Solvatomorphism (2010). *J. Pharm. Sci., 101*, 464–484.
2. Hilfiker, R. (2013). Polymorphism of Crystalline System *in Crystallization: Basic Concepts and Industrial Applications*. Weinheim, Germany: Wiley-VCH Verlag GmbH, 85–103.
3. Ghugare, P., Dongre, V., Karmuse, P., Rana, R., Sight, D., Kumar, A., Filmwala, Z. (2010). Solid state investigation and characterization of the polymorphic and pseudopolymorphic forms of indapamide. *J. Pharm. Biomed. Anal., 51* (3), 32–40.
4. Childs, S.L., Rodríguez-Hornedo, N., Reddy, L.S., Jayasankar, A., Maheshwari, C., McCausland, L., Shipplett, R., Stahly, B.C. (2008). Screening strategies based on solubility and solution composition generate pharmaceutically acceptable cocrystals of carbamazepine. *Cryst. Eng. Comm.*, *10* (7), 856.

a. Serajuddin, A.T.M. (2007). Salt formation to improve drug solubility. *Adv. Drug Deliv. Rev., 59* (7) 603–616.

5. Rubino, J., Thomas, E. (1996). Solubility, melting point and salting-out relationships in a group of secondary amine hydrochloride salts. *Int. J. Pharm., 130* (2), 179–185.
6. Mohamed, S., Tocher, A., Vickers, M., Karamertzanis, P.G., Price, S.L. (2009). Salt or Cocrystal? A New Series of Crystal Structures Formed from Simple Pyridines and Carboxylic Acids. *Cryst. Growth Des., 9* (6), 2881–2889.
7. *Polymorphism in Pharmaceutical Solids*. (2009). Edit. Brittain, H.G. New York: Informa Healthcare.
8. Boriskin, Y.S., Leneva, A., Pecheur, E.I., Polyak, S.J. (2008). Arbidol: a broad-spectrum antiviral compound that blocks viral fusion. *Curr. Med. Chem., 15* (10), 997–1005.
9. Chernyshev V. V., Davlyatshin D. I., Shpanchenko R. V., Nosyrev P.V. (2011). *Z. Kristallogr.,* 11, 832-836.
10. Orola, L., Sarcevica, I., Kons, A., Actins, A., Veidis, M. V. (2014). Conformation of the umifenovir cation in the molecular and crystal structures of four carboxylic acid salts. *J. Mol. Struct.*, *1056–1057*, 63–69.
11. Pickard, C., Mauri, F. (2001). All-electron magnetic response with pseudopotentials: NMR chemical shifts. *Phys. Rev. B., 63* (24), 245101.
12. Yates, J., Pickard, C., Mauri, F. (2007). Calculation of NMR chemical shifts for extended systems using ultrasoft pseudopotentials. *Phys. Rev. B*, *76* (2), 024401.
13. Clark, S.J., Segall, M.D., Pickard, C., Hasnip, P.J., Probert, M.I.J., Refson, K., Payne, M.C. (2005). First principles methods using CASTEP. *Z. Kristallogr.*, *220* (5/6), 567–570.
14. Harris, R.K., Hodgkinson,P., Pickard, C.J., Yates J.R., Zorin, V. (2007). Chemical shift computations on a crystallographic basis : some reflections and comments. *Magn. Reson. Chem., 45*, 174–186.
15. Perdew, J., Burke, K., Ernzerhof, M. (1996). Generalized gradient approximation made simple. *Phys. Rev. Lett.*, *77* (18), 3865–3868.
16. Childs, S.L., Stahly, G.P., Park, A. (2007). The salt-cocrystal continuum: the influence of crystal structure on ionization state. *Mol. Pharm. 4* (3), 323–338.
17. D.R. Lide (Ed.), (2006). *Handbook of Chemistry and Physics*, *87th ed.* Boca Raton, USA. CRC Press. 3-264 to 464 and 8-43 to 52.
18. Berendsen, B.J., Wegh, R.S., Essers, M.L., Stolker, A., Weigel, S. (2012). Quantitative trace analysis of a broad range of antiviral drugs in poultry muscle using column-switch liquid chromatography coupled to tandem mass spectrometry. *Anal. Bioanal. Chem.*, *402* (4), 1611–1623.
19. Socrates, G. (2004). *Infrared and Raman Characteristic Group Frequencies: Tables and Charts.* Chichester, GB: John Wiley & Sons.

20. Madarász, J., Bombicz, P., Jármi, K., Bán, M., Gál, S., Pokol, G. (2002). Thermal, FTIR and XRD study on some 1:1 molecular compounds of theophylline. *J. Therm. Anal. Calorim.*, *69* (1), 281–290.
21. Stevens, J.S., Byard, S.J., Muryn, C., Schroeder, S.L.M. (2010). Identification of protonation state by XPS, solid-state NMR, and DFT: characterization of the nature of a new theophylline complex by experimental and computational methods. *J. Phys. Chem. B*, *114* (44), 13961–13969.
22. Apperley, D.C., Markwell, F., Harris, R.K., Hodgkinson, P. (2012). NMR characterisation of structure in solvates and polymorphs of formoterol fumarate. *Magn. Reson. Chem.*, *50* (10), 680–690.
23. Harris, R.K., Hodgkinson, P., Pickard, C.J., Yates, J.R. (2009). Chemical Shift Computations for Crystalline Molecular Systems: Practice. *eMagRes.*
24. Chierotti, M.R., Gobetto, R. (2008). Solid-state NMR studies of weak interactions in supramolecular systems. *Chem. Commun., 14,*1621–1634.
25. Li, Z.J., Abramov, Y., Bordner, J., Leonard, J., Medek, A., Trask, A.V. (2006). Solid-state acid-base interactions in complexes of heterocyclic bases with dicarboxylic acids: crystallography, hydrogen bond analysis, and 15N NMR spectroscopy. *J. Am. Chem. Soc.*, *128* (25), 8199–8210.
26. Gould, P.L. (1986). Salt selection for basic drugs. *Int. J. Pharm., 33* (1–3), 201–217.
27. O'Connor, K.M., Corrigan, O.I. (2001). Preparation and characterisation of a range of diclofenac salts. *Int. J. Pharm*., 226 (1–2), 163–179.
28. Black, S.N., Collier, E.A., Davey, R.J., Roberts, R.O.N.J. (2007). Structure , solubility , screening , and synthesis of molecular salts. *J. Pharm. Sci., 96* (5), 1053–1068.

UMIFENOVIRA UN DIKARBONSKĀBJU VEIDOTO MOLEKULĀRO KOMPLEKSU RAKSTUROŠANA UN FIZIKĀLĶĪMISKO ĪPAŠĪBU NOTEIKŠANA

A. Kons, A. Bērziņš, K. Krūkle-Bērziņa, A. Actiņš

K O P S A V I L K U M S

Apskatīti trīs umifenovira un dikarbonskābju veidotie molekulārie kompleksi, kas iegūti, lai uzlabotu zāļu biopiejamību. Visi trīs iegūtie savienojumi pētīti ar pulveru rentgendifraktometriju, infrasarkano spektroskopiju un cietvielu magnētiskās rezonanses spektroskopiju, kā arī noteikta šo savienojumu šķīdība un termiskās īpašības. Veikti polimorfo un pseidopolimorfo formu meklējumi, kristalizējot molekulāros kompleksus no dažādiem šķīdinātājiem un tos kopsamaļot gar ar, gan bez šķīdinātāja piedevas.

Iesniegts10.09.2012.